Supporting Information

1. Experimental

All chemicals reagents in this study were of analytic grade and used directly without further treatment. Multiwall carbon nanotubes (diameter: 10-20 nm, length: 10-30 μm) were purchased from Chengdu Time Nano (Sichuan, China).

1.1 Materials synthesis

1.1.1 Pretreatment of raw materials

Coal-based microcrystal (CMC) can be prepared from needle coke by acid treatment. 3 g needle coke powder was carefully added into a beaker with 75 mL concentrated sulfuric acid (98%) under the ice bath. Subsequently, 12 g potassium permanganate was added into the above solution slowly and followed by stirring for 6 h at room temperature. Then, 135 mL deionized water was poured into the beaker and heated up to 60 °C with stirring overnight. Finally, the CMC was obtained after centrifugal washing and drying.

5 g CNT was placed in a flask containing 120 mL mixed acid of 30 wt% HNO_3 and 49 wt% H_2SO_4 (1: 3, volume ratio), and kept stirring at 80 °C for 12 h. The functionalized CNT was obtained after washing to neutral by filtration.

1.1.2 Preparation of CMC/CNT composites

The treated needle coke powders and 10 mg of CNT were added into a beaker with distilled water to form a 1mg mL^{-1} mixed solution by ultrasonic treatment for 90 minutes. Binder-free electrode was prepared by depositing the mixed solution on the Cu foil and dried at 70 °C in vacuum oven. The four samples were marked as 2CMC/CNT, 3CMC/CNT, 4CMC/CNT and 5CMC/CNT, corresponding to 20 mg, 30 mg, 40 mg and 50 mg CMC, respectively. For comparison, pure CNT electrode was also prepared by solution deposition of CNT dispersion.

1.1.3 Materials characterization

The crystal structure was characterized by X-ray diffraction (XRD, MiniFlex600) using Cu Kα radiation (λ=0.1541 nm) over a 2θ range of 5-80 degree. The morphology was characterized by scanning electron microscopy (SEM, JSM-7001F). The surface functional groups were analyzed by Fourier transformed infrared spectroscopy (FTIR, Nicolet IS50) and X-ray photoelectron spectroscopy (XPS, Escalab 250Xi). Thermal gravimetry-mass spectrometry (TG-MS) measurement was conducted on a Thermogravimetric analyzer (Setaram Setsys Evolution 16/18) connected with Mass spectrometry (Pfeiffer Omni star) with a heating rate of 5 °C/min under argon atmosphere (50 mL/min). The test of Brunauer-Emmett-Teller (BET) surface area was conducted by nitrogen absorption apparatus (Beishide 3H-2000 PS2).

1.1.4 Electrochemical measurements

After drying at 100 °C in a vacuum oven overnight, the CMC/CNT on Cu foil was directly used as an anode for 2025-type button cells. The loading mass of active material on the Cu foil was ~1.0 mg cm^{-2}. The half cells were assembled in an Ar-filled glove box, which consist of sodium metal as counter electrode, Whatman glass fiber as separator, and 1 M NaClO$_4$ in a mixture of EC and PC (1:1 = v:v) with 5% (volume) FEC as the ester-based electrolyte.

Cyclic voltammetry (CV) curves were recorded on the electrochemical work station (CHI1000C, China) in the range of 0.01-3.0 V. Galvanostatic cycling performance and rate capability were investigated by a battery test station (Land 2001A, China) in the voltage range of 0.01-3.0 V. And the electrochemical impedance spectra (EIS) were collected by the electrochemical work station (CHI660E, China) with an AC signal amplitude of 5 mV at a frequency range of 0.1 Hz-100 kHz.
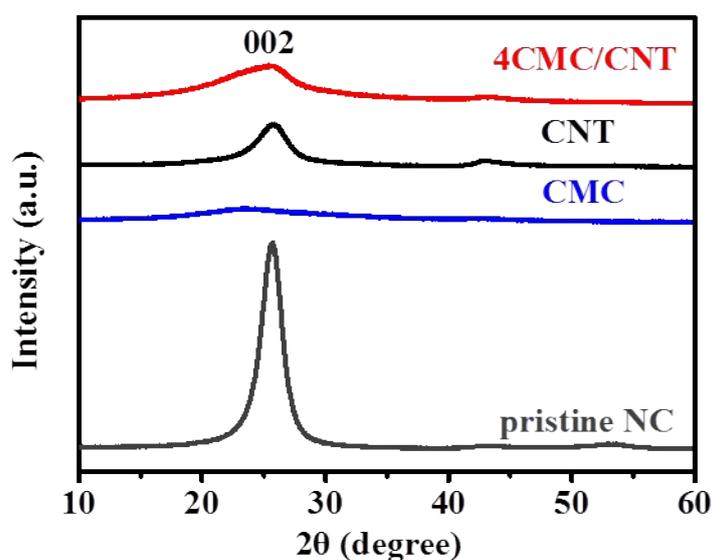
Figure S1 XRD patterns of pristine NC, CMC, CNT and 4CMC/CNT
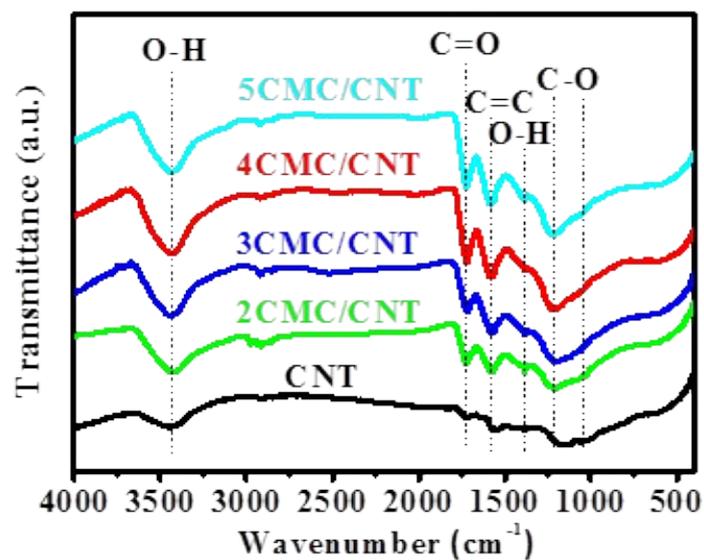
Figure S2 FT-IR spectra of all samples

As shown in Figure S2, the oxygen-containing functional groups of the samples were characterized by FT-IR spectra. The stretching vibrations of hydroxyl groups (O–H, 3430 cm^{-1}), carbonyl and carboxylic groups (C=O, 1730 cm^{-1}), C=C (1580 cm^{-1}), C–O (1212 cm^{-1} and 1040 cm^{-1}) and the O–H bending deformation in carboxylic acid (O–H, 1390 cm^{-1}) were observed.
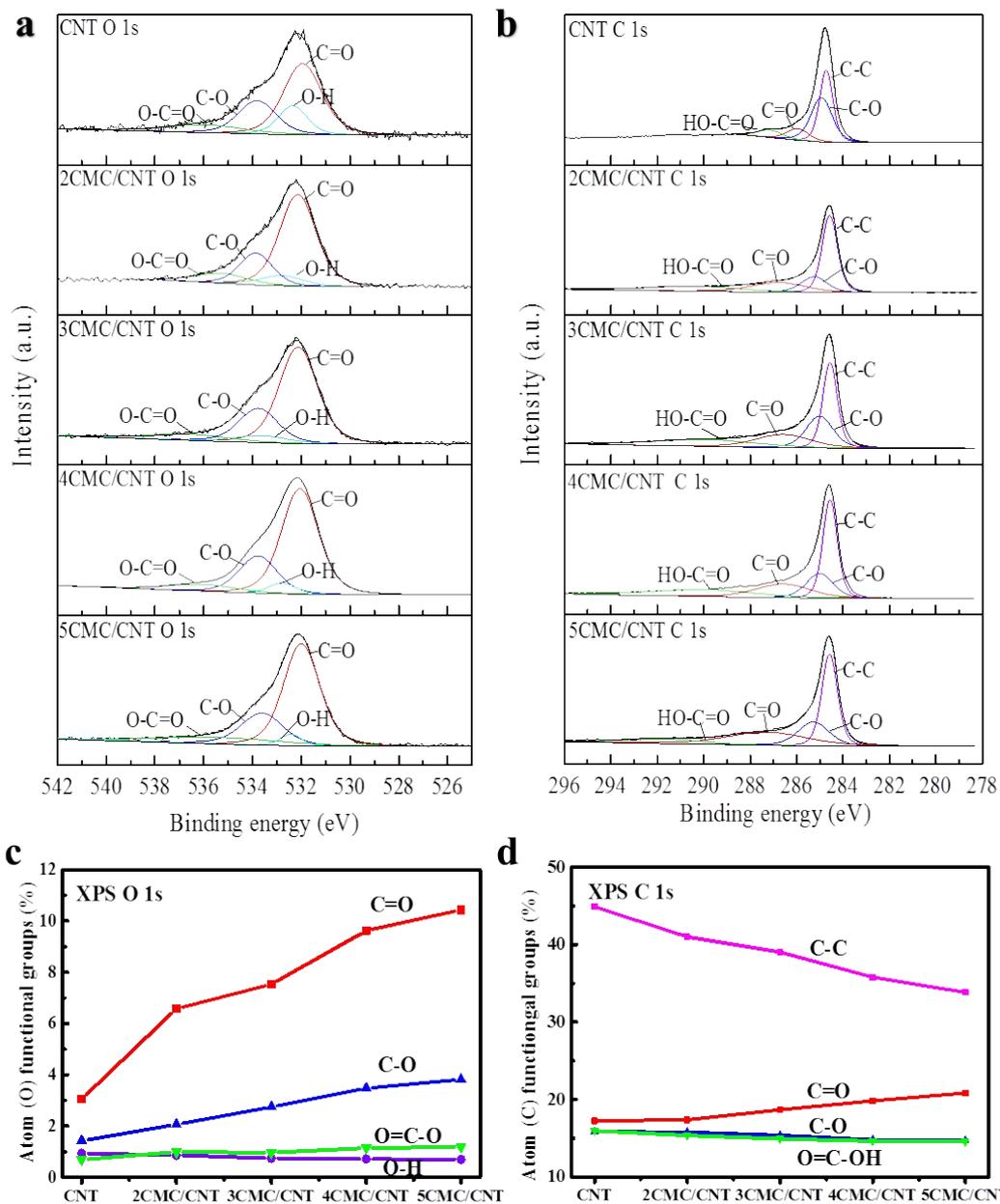
Figure S3 High-resolution XPS spectrum of all samples for (a) C1s and (b) O1s, (c) Atom O and

(d) C functional groups percentage calculated by XPS analysis results for all samples.

The oxygen functional groups in functional CMC/CNT composites and CNT were

investigated by XPS. As shown in S 3a, the O 1s spectra deconvoluted into four peaks

for oxygen-containing functional groups, which could be ascribed to C=O (531.9 eV),

O–H (532.3 eV), C–O (533.8 eV) and O=C–OH (535.9 eV), respectively.[1] As shown

in Fig. S 3b, the C 1s spectra exhibit four peaks by peaks fitted, located at 284.6, 285.4,

287.1 and 290.8 eV, which could be assigned to C–C, C–O, C=O and O=C–O,

respectively.[2] The percentages of C and O functional groups of all samples based on

the fitted XPS spectra was shown in Fig. S 3c and S 3d.
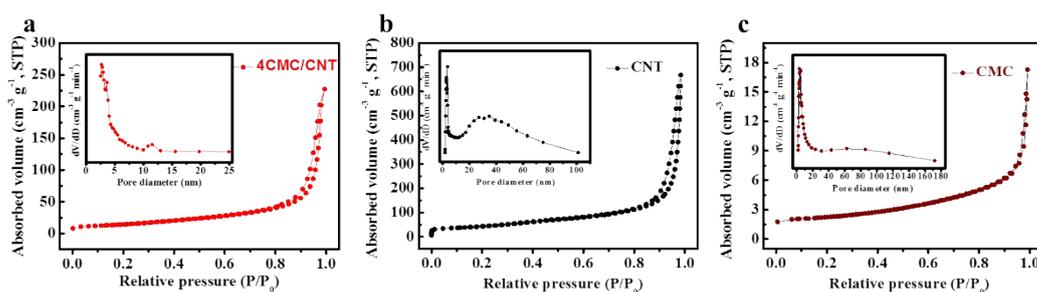
Figure S4 N2 adsorption/desorption isotherm and the inset is the pore size distribution of (a) 4CMC/CNT, (b) CNT, (c) CMC.

The BET surface areas and pore size distributions of CMC, CNT, 4CMC/CNT

were assessed by using N_2 adsorption and desorption isotherms. As depicted in Figure

S4, three samples present the typical type IV isotherms along with hysteresis loops.

CMC, CNT, 4CMC/CNT exhibit a specific surface area of 7.4, 158 and 53.3 m^2 g^{-1},

respectively. The pore size distributions indicate that there is large quantities of

mesopores in these materials.
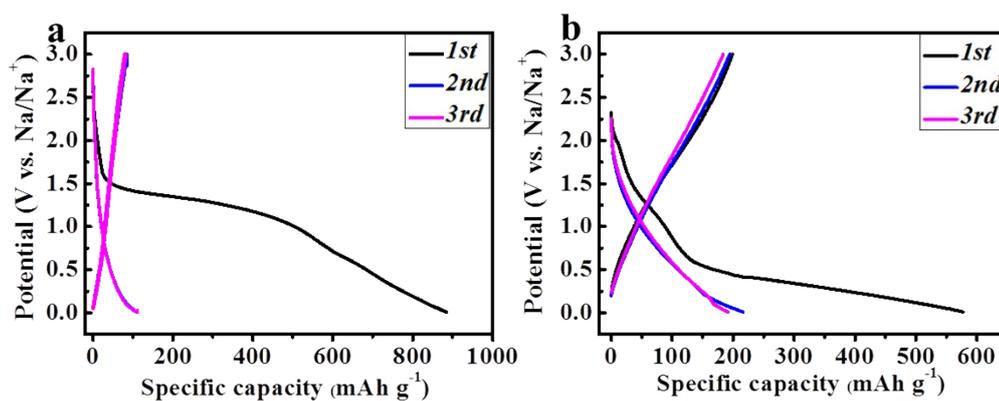
Figure S5 Galvanostatic discharge/charge curves at 0.05 A g^{-1} of (a) CNT and (b) CMC at a voltage of 0.01-3.0 V.

Initial discharge/charge capacities of 884.8/85.2 mA h g^{-1} with ICE of 9.6% for CNT, and 577/198.7 mA h g^{-1} with ICE of 34.4% for CMC are obtained in the galvanostatic discharge/charge curves (Figure S5) at 0.05 A g^{-1}. The ICE of CMC is similar with most carbons in the references, because the ICE is mainly related to the side reaction from the commercial binder PVDF. The low ICE of CNT might be attributed to the high surface area and irreversible surface reaction. Comparably, the 4CMC/CNT composite exhibiting high ICE due to the absence of commercial binder and appropriate specific surface area.
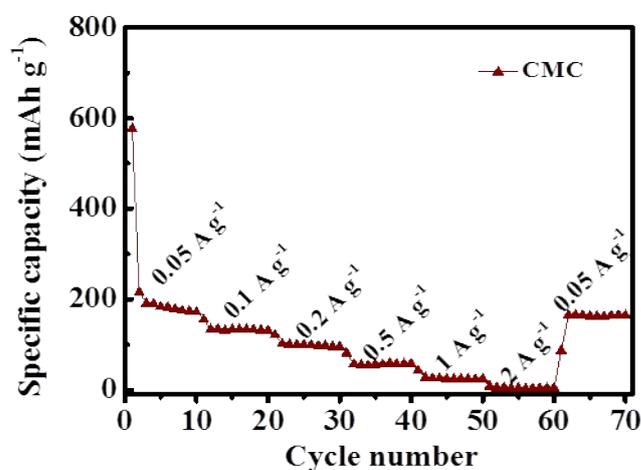
Figure S6 Rate performance from 0.05 A g^{-1} to 2 A g^{-1} for CMC
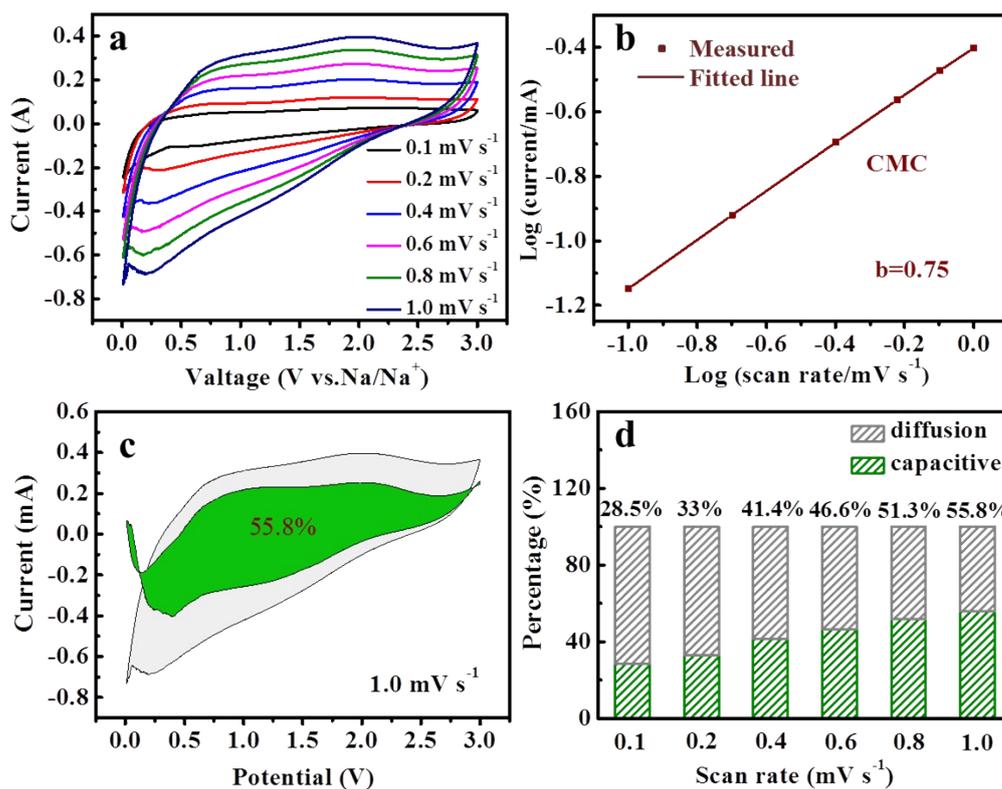
Figure S7 Kinetic analysis for CMC electrode (a) CV curves at various scanning rates from 0.1 mV s^{-1} to 1.0 mV s^{-1}, (b) Logarithmic current versus logarithmic scan rate plots (b value is calculated), (c) Capacitance contribution percentage at 1.0 mV s^{-1}, (d) Contribution percentage of capacitive and diffusion-controlled charge under different scan rates.

Supplementary References

1   Y. Joon, J. Joon, Y. Il, J. Kook, H. Na, J. Kim and S. Bin, Electrochim. Acta, 2014, **116**, 118–128.

2   H. R. Byon, B. M. Gallant, S. W. Lee and Y. Shao-horn, Adv. Funct. Mater., 2013, **23**, 1037–1045.